Journal of Applied Polymer Science

Preparation of Electrospun Silk Fibroin Nanofibers from Solutions Containing Native Silk Fibrils

Zhi Liu,[1] Feng Zhang,[2] Jinfa Ming,[1] Shiyu Bie,[1] Junjuan Li,[1] Baoqi Zuo[1]

[1]National Engineering Laboratory for Modern Silk, College of Textile and Clothing Engineering, Soochow University, Suzhou 215123, China

[2]Jangsu Province Key Laboratory of Stem Cell, Medical College of Soochow University, Suzhou, 215123, China

Correspondence to: B. Zuo (E-mail: bqzuo@suda.edu.cn)

ABSTRACT: Electrospinning solutions containing native silk fibrils with varied diameter and length were firstly achieved by dissolving silk in $CaCl_2$/Formic acid solvents. The structure of nanofibrils significantly improved the spinnability of electrospinning solution. The diameter of electrospun silk fibroin (SF) nanofibers increased from 40 nm to 1.8 μm, which could be achieved through increasing the solution concentration from 2 to 10%, implying a good size control over a wide range in this process. The structure of SF nanofibers transferred from random coil to beta-sheet, before and after ethanol treatment, respectively. The mechanical properties of the SF nanofibers were improved significantly with stress and strain at break of 11.15 MPa and 7.66% in dry state, and 3.32 MPa and 174.0% in wet state. The strategy for preparing SF nanofibers with improved mechanical properties and fiber diameter control over a wide range provides benefits for the application of this material. © 2014 Wiley Periodicals, Inc. J. Appl. Polym. Sci. **2015**, *132*, 41236.

KEYWORDS: biomaterials; cellulose and other wood products; electrospinning; membranes; plasticizer

Received 3 March 2014; accepted 6 June 2014

DOI: 10.1002/app.41236

INTRODUCTION

Bombyx mori silk with exceptional taking performance has been used in textiles for thousands of years in human history. As a part of silk, silk fibroin (SF) offers a series of excellent properties including mechanical superiority and biocompatibility, which makes SF great potential applications in biological fields in recent years, especially in tissue engineering,[1,2] wood dressing,[3] and drug release systems.[4,5] After dissolving SF in solvents to obtain a regenerated solution, the power, fiber, and film of regenerated SF are obtained through various processes. In these processes, electrospinning offers a unique superiority for preparing protein-based biomaterials with controllable nanofibrous structure. Accompanying the biocompatibility and spinnability of silk fibroin, electrospun SF nanofibers have been investigated widely for potential applications in tissue engineering. However, the electrospun SF nanofiber mats showed poor mechanical properties, which limited its further applications in tissue engineering.

Traditionally, in order to improve the mechanical properties of electrospun SF nanofibers, the following methods were carried out. One is to treat SF nanofibers with organic solvent to induce structural transition from random to β-sheet structure.[6] The second is to add a reinforcing agent into the spinning solution to prepare composite fibers, such as carbon nanotubes, multiwalled carbon nanotubes.[7,8] The third is to treat SF nanofibers with crosslinking agent.[9,10] These methods are effective to some extent to enhance the mechanical properties of SF nanofibers. As is known to all, native silk has outstanding mechanical properties, which is origin from its hierarchical nanofibrous structure.[11–14] Usually, the nanofibril structure is completely decomposed to molecules during silk dissolution in traditional solvent, such as LiBr aqueous solutions and $CaCl_2$/C_2H_5OH/H_2O solutions. And SF nanofibers obtained from self-assembly, which is a process from decomposition to restructuring, resulting in the poor mechanical properties of regenerated silk materials. What's more, the process of the SF nanofibril formation is complex, time-consuming and sensitive to environmental conditions.[15] Recently, nanofibers extracting directly from natural materials by physical or chemical method has been proved an effective way to generate high strength materials.[16] The native nanofibril would be very useful for constructing high performance silk-based materials if we could preserve this structure during regeneration process.

Formic acid (FA) can not dissolve native silk at all. However, the adding of a small quantity of inorganic salts into FA makes it an effective solvent for dissolving degummed silk.[17] Unfortunately, the merits of this method have not been realized and developed sufficiently. In this study, we first employed $CaCl_2$/Formic acid ($CaCl_2$/FA) system to dissolve silk while preserving

Table I. Sample Codes of Four Concentrations of $CaCl_2$

Sample	$CaCl_2$ (%)	FA (%)	Dissolution time(min)
1	1	99	600
2	2	98	40
3	5	95	30
4	10	90	25

the native nanofibril structure. The effect of different nanofibril structure on rheological properties, spinnability of electrospinning solution, and the morphology, secondary structure, and mechanical properties of electrospun SF nanofibers were extensively investigated. What's more, the residual of $CaCl_2$ in SF nanofibers was confirmed by XPS.

EXPERIMENTAL

Materials

Bombyx mori silk was supplied from the city of Tong Xiang (Zhejiang, China). Sodium carbonate, Calcium chloride anhydrous, formic acid, and ethanol were purchased from Sinopharm Chemical Reagent China (Shang Hai, China).

Preparation of Regenerated SF Films

Bombyx mori silk was boiled for 60 min in an aqueous solution of Na_2CO_3 with concentrations of 0.05% (w/v) and then rinsed thoroughly with distilled water to extract the sericin proteins. The dried degummed silk was then directly dissolved in $CaCl_2$/FA for 3h at room temperature to prepare 6% w/v silk solution. Table I lists the sample code and its dissolution conditions. The dissolution time of silk is sensitive to $CaCl_2$ concentration, which decreased from 600 min to 40 min when increasing $CaCl_2$ concentration from 1 to 2%.

Then the SF/$CaCl_2$/FA solutions were cast on polystyrene Petri dishes to prepare SF films. After dried, the SF films were immersed in deionized water to remove the $CaCl_2$ for 10 h, and then dried in air.

Preparation of Electrospun SF Nanofibers

The electrospinning solutions were prepared by dissolving the regenerated SF films above in FA for 3 h. A high electric potential of 12 kV was applied to a droplet of SF solution at the tip of a syringe needle (0.8 mm in internal diameter). The electrospun nanofibers were collected on flat aluminum foil which was placed at a distance of 10 cm from the syringe tip. A constant volume flow rate of 1 mL/h was maintained using a syringe pump. For post-treatment, the electrospun SF nanofibers were immersed in 75% (v/v) ethanol for 1 h and then dried in air. The thickness of the obtained regenerated SF mats is from 48 to 92 μm.

Measurement and Characterization

The morphology of nanofibrils in solution (1 μL SF/FA solution was dropped on silica plate, and was left to dry) and electrospun fibers was observed using an SEM (Hitachi S-4800, Tokyo, Japan) at 20°C, 60 RH. Samples were sputter-coated with gold layer prior to imaging. The diameters of nanofibers were calculated by measuring at least 100 fibers at random using Image *J*.

Rheological studies were run on a rheometer (Rheometer, TA Instruments, New Castle, DE) with a 35 mm cone plate (Ti, 35/1°). The normal force applied on the sample during lowering of the top

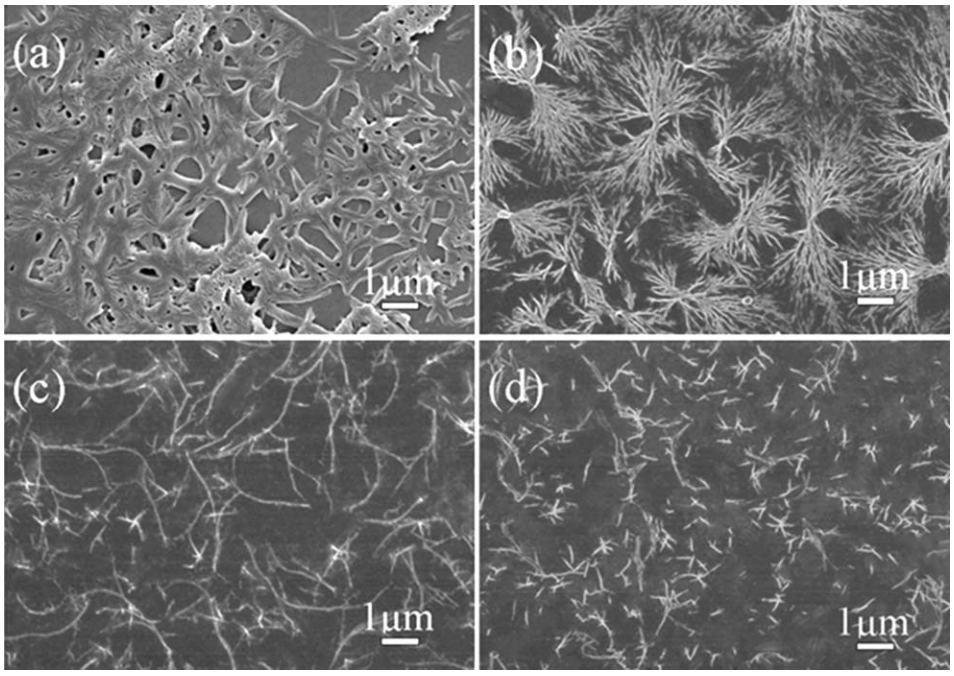

Figure 1. SEM images of SF state in the electrospinning solutions prepared by dissolving 1% $CaCl_2$-film (a), 2% $CaCl_2$-film (b), 5% $CaCl_2$-film (c), and 10% $CaCl_2$-film (d) in formic acid.

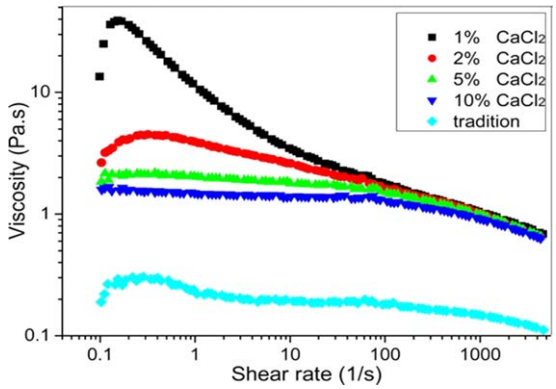

Figure 2. Rheological behaviors of 6 wt % SF solutions prepared by dissolving 1% $CaCl_2$-film, 2% $CaCl_2$-film, 5% $CaCl_2$-film, 10% $CaCl_2$-film, and $CaCl_2/C_2H_5OH/H_2O$-film (tradition) in formic acid. [Color figure can be viewed in the online issue, which is available at wileyonlinelibrary.com.]

plate was limited to 0.1*N*. The shear rate was linearly increased from 0.1 to 5000 1/s at 25°C.

FTIR spectra were obtained using a Magna spectrometer (NicoLET 5700, USA) in the spectral region of 400–4000 cm^{-1}. The powder of electrospun SF mats was pressed into potassium bromide (KBr) pellets prior to data collection.

X-ray diffraction (X'PERT PRO MPD. PANalytical Company, kyoutofu, Tokyo) was operated at 40 kV tube voltage and 40 mA tube current. CuK_α radiation was used with diffraction angle $2\theta = 2°–45°$, the scanning rate is 2°/min with powdered electrospun SF mats.

The mechanical properties of electrospun SF nanofibre mats (10 mm × 40 mm) were obtained using a universal texting machine (Instron 3365, Instron, Norwood, MA) (gauge length: 20 mm; cross-head speed: 0.2 mm/s) at 25 ± 0.5°C, 60 ± 5% relative humidity. The thickness of the mats was measured using a micrometer. At least five measurements for each sample were performed in the testing.

The surface chemical compositions of electrospun SF mats were analyzed by SHIMADZU/KRATOS X-ray photoelectron spectrometer (XPS) to determine whether the $CaCl_2$ were removed completely. The incident angle of the X-rays was 90°, and the vacuum degree of the analysis chamber was less than or equal to 1×10^{-9} Pa. All the deviations of the binding energy in the XPS measurement were corrected by the carbon (C1s) photoelectron emission signal occurring at 284.5 eV.

Statistical Analysis

All values were expressed as mean ± standard deviation. Statistical differences were determined by a Mann-Whitney U test (Independent *t* test, SPSS).

RESULTS AND DISCUSSION

Morphology of SF in Electrospinning Solutions

The states of SF in electrospinning solution were observed by SEM, as shown in Figure 1. The diameter and length of fibers decreased with the increased content of $CaCl_2$. It can be seen that nanofibrils aggregated together, forming bunches of fibers [Figure 1(a)]. And plenty of nanofibrils were observed, 20–80 nm in diameter. They aggregated together through a node (the closer to the node, the bigger diameter of SF) [Figure

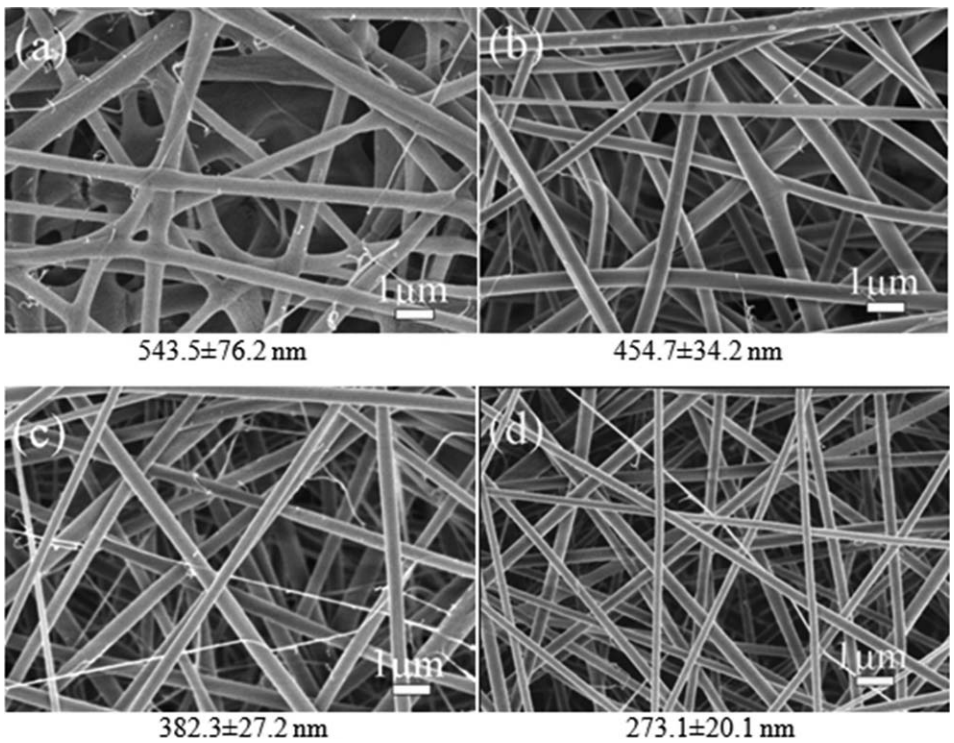

Figure 3. SEM images of SF nanofibers electrospun from 6 wt % SF solutions prepared by dissolving 1% $CaCl_2$-film (a), 2% $CaCl_2$-film (b), 5% $CaCl_2$-film (c), and 10% $CaCl_2$-film (d) in formic acid.

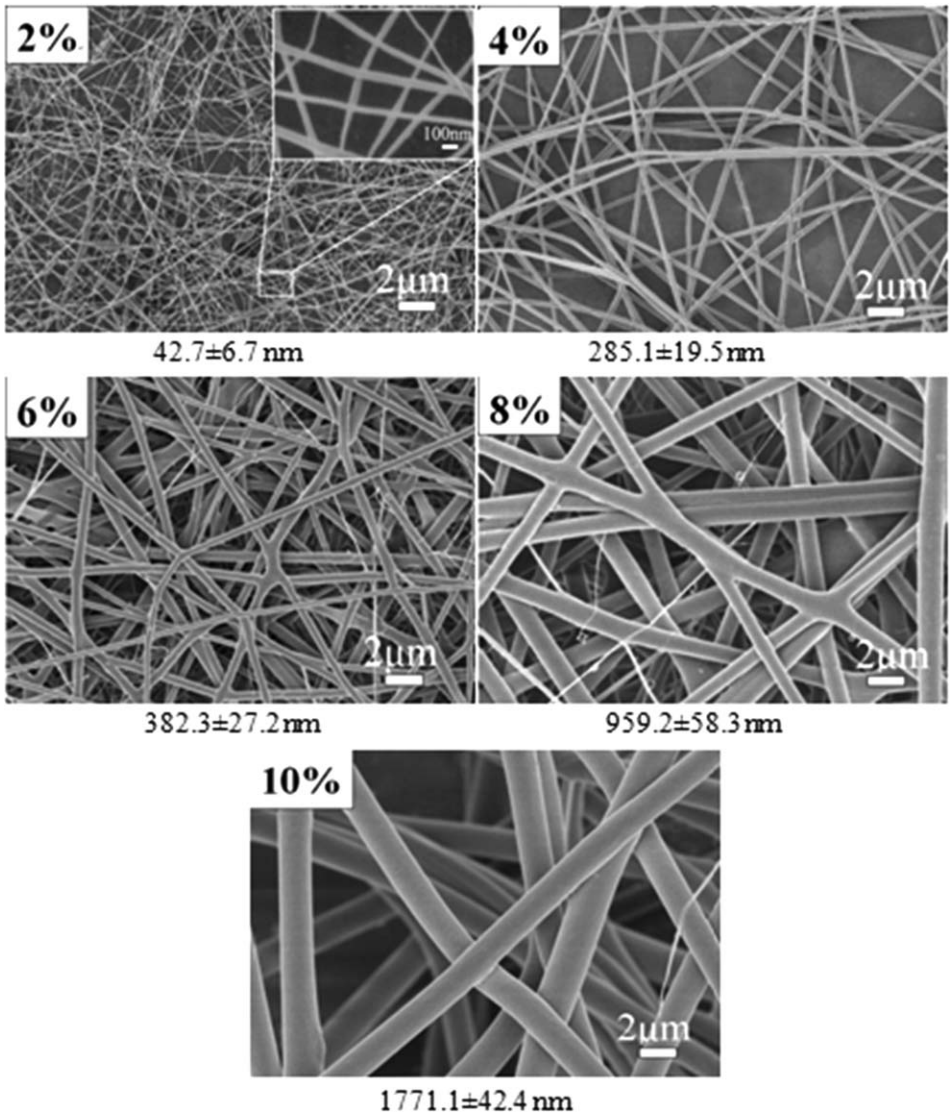

Figure 4. SEM images of SF nanofibers electrospun from SF solutions with 2%, 4%, 6%, 8%, and 10% concentrations.

1(b)]. As the $CaCl_2$ contents increase, all the nanofibrils dispersed in single state, about 1–5 μm in length and about 30 nm in diameter [Figure 1(c)]. At last, the length was shortened, but the change of diameter was not obvious, as shown in Figure 1(d). From the results observed, we can see that silk nanofibrils obtained in dissolving process, and we could clearly know the change of SF nanofibrils as the increase of $CaCl_2$ content. The nanofibrils with diameters of 20–170 nm are important components in the hierarchical structure of native silk fiber. It is observed that nanofibrils were preserved when $CaCl_2$/FA was employed to dissolve silk. The morphology of the resulting nanofibril can be tuned by simply altering the concentration of $CaCl_2$, in which regenerated SF showed smaller diameter and shorter length with the increase of $CaCl_2$ concentration.

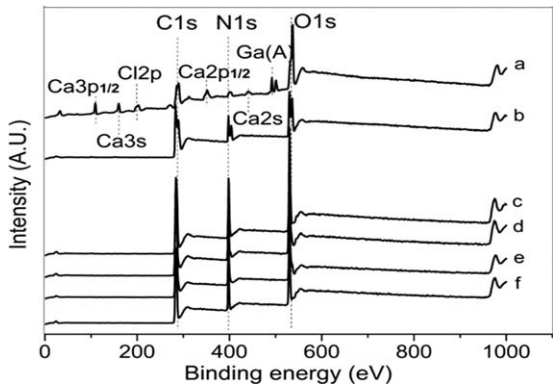

Figure 5. XPS survey scan spectra of SF film before (a) and after (b) water rinsing and electrospun SF mats from 1% $CaCl_2$-film (c), 2% $CaCl_2$-film (d), 5% $CaCl_2$-film (e), and 10% $CaCl_2$-film (f).

Rheological Behavior of Electrospinning Solutions

The rheological behavior is closely related to the spinnability of polymer solution, and is also an indicator for protein aggregates structure in solution.[18] Therefore, we investigated the rheological behavior of SF solutions prepared by using $CaCl_2$/FA system and $CaCl_2/C_2H_5OH/H_2O$ system (termed as Tradition) (Figure 2). Clearly, the viscosity measurements over a range of shear

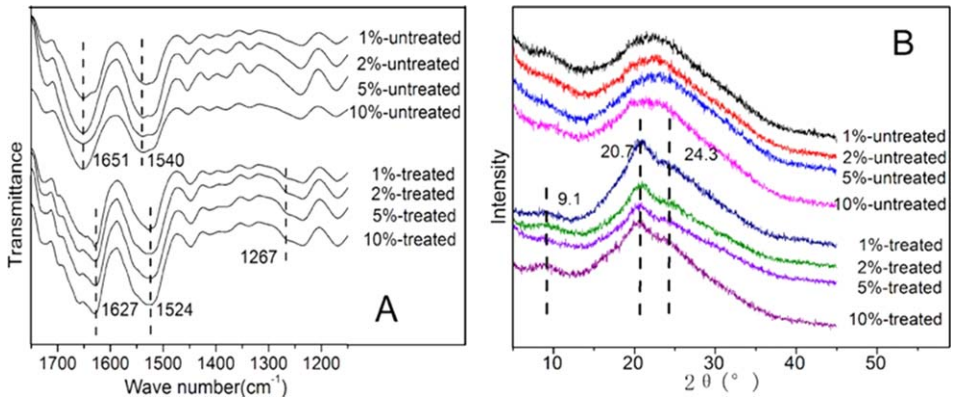

Figure 6. FTIR (a) and XRD (b) spectra of SF nanofibers electrospun from 6 wt % SF solutions prepared by dissolving 1% $CaCl_2$-film, 2% $CaCl_2$-film, 5% $CaCl_2$-film, and 10% $CaCl_2$-film in formic acid. [Color figure can be viewed in the online issue, which is available at wileyonlinelibrary.com.]

rates confirmed the vast differences between these two systems (Figure 2). Over the range of shear rates tested, the tradition solution flowed undisturbed and behaved like Newtonian fluids with significantly low viscosity, in agreement with previous findings.[19,20] In contrast, the new system exhibited shear-thickening before the onset of shear-thinning with significantly higher viscosities which is similar to that of natural silk dopes.[19] At low shear rates, the nanofibril entangled with each other, resulting in the increased viscosities, and shear-thickening behavior. Besides, the shear-thickening behavior was significantly dependent on the $CaCl_2$ concentration which dissembled silk into nanofibril with different diameter and length (Figure 1). The nanofibril entanglement would be weakened due to the reduced diameter and length of silk nanofibrils. In addition, the shear-thinning behavior was also observed at high shear rates likely due to the orientation of the nanofibrils. Despite the same origin of the reconstituted protein from native silk, the dissolution process did substantially destroy the silk hierachical structure at different nanoscale level, which in turn affected the solution properties.

Morphology and $CaCl_2$ Residual of Electrospun Silk Fibers

The morphology and diameters of the electrospun SF nanofibers were examined by SEM, as shown in Figure 3. The fiber formation was closely related to the protein aggregate structure in spin solution. All silk solutions produced sub-micrometer fibers with less than 600 nm average diameter. The fiber diameter decreased from 543 nm to 273 nm as $CaCl_2$ concentration increased from 1 to 10%. The higher concentration of $CaCl_2$ resulted in the nanofibril with smaller diameter and short length, which makes the regenerated SF nanofibers with smaller diameter.

To further investigate the spinnability, the solution containing silk nanofibrils was diluted to different concentrations, 10%, 8%, 6%, 4%, and 2%. Figure 4 shows SEM micrographs of electrospun SF nanofibers derived from different solution concentrations. All exhibits good spin ability, even at low concentration of 2%, which was impossible in previous reports.[21–23] With the increase of silk fibroin concentration from 2 to 10%, the diameter of electro spun Nan fibers increased from 42 nm to 1771 nm. The good spin ability of these solutions indicated the important role of silk structure in electrospinning solutions. Moreover, the results demonstrated the feasibility of fiber size control over a wide range in such system.

In addition, we employed XPS to confirm the complete removal of $CaCl_2$ in the resulting silk Nan fibers. As shown in Figure 5, all samples shared same three separated peaks which correspond to C1s (285eV), N1s (403eV), and O1s (532eV).[24] The obvious

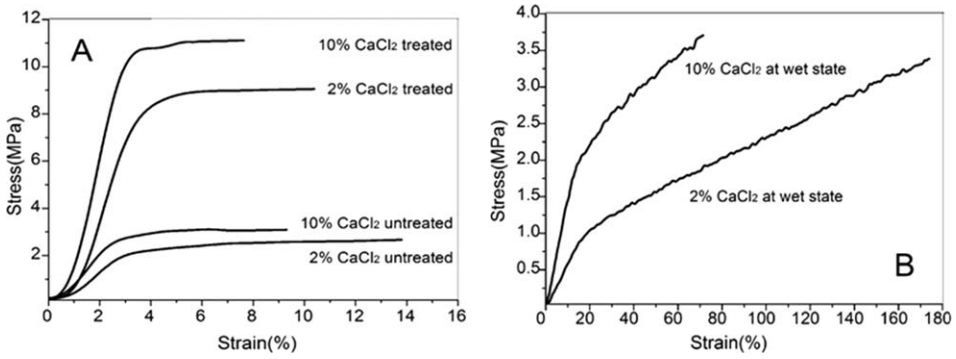

Figure 7. Mechanical properties of electrospun SF nanofiber mats before and after treated in dry state (a). Mechanical properties of electrospun SF nanofiber mats after treated in wet state (b).

Table II. Mechanical Properties of Electrospun SF Nanofiber Mats

Sample	Rupture stress (MPa)	Strain (%)
2% $CaCl_2$ untreated	2.67 ± 0.60	13.80 ± 1.64
2% $CaCl_2$ treated	8.90 ± 0.41	10.40 ± 1.08
2% $CaCl_2$ wet state	3.32 ± 0.10	174.00 ± 18.5
10% $CaCl_2$ untreated	2.97 ± 0.37	9.32 ± 1.01
10% $CaCl_2$ treated	11.15 ± 1.04	7.66 ± 1.42
10% $CaCl_2$ wet state	3.74 ± 0.14	71.74 ± 8.10
RSF mats treated[33]	1.49	1.63

existing of $CaCl_2$ was detected in the silk film without rinsing in deionizer water, which had peaks correspond to $Ca3p_{1/2}$ (108eV), Ca3s (160eV), Cl2p (199eV), $Ca2p_{1/2}$ (350eV), Ca2s (439eV), Ca (A) (490eV). However, these peaks disappeared in the water rinsed film and electro spun Nan fibers [Figure 5(b–f)], suggesting the complete removal of $CaCl_2$ during film water rinsing process.

Secondary Structure of Electro Spun Silk Fibers

The secondary structure of electro spun SF Nan fiber was determined by FTIR and XRD (Figure 6). The as-spun SF Nan fiber showed two absorption peaks with a center around 1651 cm^{-1} (amide I) and 1540 cm^{-1} (amide II) [Figure 6(a)], corresponding to random coil and or helical conformation.[25–27] To improve stability in water, the SF Nan fibers were treated with 75% ethanol to induce the structural transition to silk II with the characteristic adsorption peaks at 1627 cm^{-1}, 1524 cm^{-1}, and 1267 cm^{-1} (amide III) [Figure 6(a)].[28,29] This structural transition of SF Nan fiber from silk I to silk II was also confirmed by XRD analysis [Figure 6(b)]. It showed that diffraction peaks at 21° (a broad peak) before treatment, and the treated electro spun SF Nan fiber exhibited three diffraction peaks at 9.1°, 20.7°, and 24.3°, indicating the transition from silk I to silk II.[30] These results suggested that the existence of native silk fibrils in solutions has no obvious effect on secondary structure of regenerated SF mats.

Mechanical Properties of Electrospun Silk Fibers

The mechanical properties of electrospun SF nanofiber mats were tested, since it was a key factor for applications in tissue engineering. The typical stress−strain curves of electrospun SF nanofiber mats are shown in Figure 7. The strength and breaking strain are shown in Table II. It can be seen that the mechanical properties of SF mats was affected faintly by the $CaCl_2$ concentration. And it was improved significantly by the ethanol treatment due to the formation of β-sheet structure, in agreement with previous reports.[6,31] The stress and strain at break of SF nanofibers mats were 11.15 MPa, 7.66% in dry state. These results were superior the reported 0.82 MPa, 0.76%[32] and 5.6 MPa, 5.0% (mats thickness 30 μm).[6] Besides, the strength and strain at break of SF nanofiber mats in wet state were 3.32 MPa, and 174%, which were close to the reported 4.02 MPa, 149%,[33] and 3.46 MPa, 127.8%[34] for regenerated SF films after treatment. Recent study confirmed the role of self-assembly silk nanofibers in improving the flexibility of regenerated silk films[35] and nanofiber mats.[36] Therefore, it is believed that the improvement of the mechanical properties of electrospun SF nanofiber mats, especially in wet state, was likely due to the preserved nanofibrils in electrospinning solutions.

CONCLUSIONS

Native silk fibrils were obtained from $CaCl_2$/FA system. As a part of nature silk components, native silk fibrils make the electrospinning solutions having many good qualities. Interestingly, the regenerated SF solutions exhibited high viscosities, which made it possible in low SF concentration to electrospinning, and just 2 wt % SF solutions showed good spinnability. What's more, the diameter of SF nanofibers showed a good size control from 42 nm to 1771 nm through sample adjustment of SF concentration, implying more applications in the future. The secondary structure transferred from random structure to more crystalline structure after ethanol treated. To our pleasure, the electrospun SF mats exhibited improved mechanical properties, the stress at break, up to 11.15 MPa after treated, especially the excellent strain property, up to 174%, at wet state. The regenerated SF nanofibers with a good size control and good mechanical properties make it great potential applications in biological field, not only in tissue engineering but also in drug delivery and wound dressing.

ACKNOWLEDGMENTS

We are gratefully acknowledged the support of the First Phase of Jiangsu Universities' Distinctive Discipline Development Program for Textile Science and Engineering of Soochow University, the National Natural Science Foundation of China (81271723).

REFERENCES

1. Patra, C.; Talukdar, S.; Novoyatleva, T.; Velagala, S. R.; Muhlfeld, C.; Kundu, B.; Kundu, S. C.; Engel, F. B. *Biomaterials* **2012**, *33*, 2673.
2. Goh, Y. F.; Shakir, I.; Hussain, R. *J. Mater. Sci.* **2013**, *48*, 3027.
3. Shang, S. M.; Zhu, L.; Fan, J. T. *Carbohydr. Polym.* **2013**, *93*, 561.
4. Hofer, M.; Winter, G.; Myschik, J. *Biomaterials* **2012**, *33*, 1554.
5. Chen, M. J.; Shao, Z. Z.; Chen, X. *J. Biomed. Mater. Res. A* **2012**, *100*, 203.
6. Cao, H.; Chen, X.; Huang, L.; Shao, Z. Z. *Mater. Sci. Eng. C* **2009**, *29*, 2270.
7. Gandhi, M.; Yang, H.; Shor, L.; Ko, F. *Polymer* **2009**, *50*, 1918.
8. Ayutsede, J.; Gandhi, M.; Sukigara, S.; Ye, H. H.; Hsu, C. M.; Gogotsi, Y.; Ko, F. *Biomacromolecules* **2006**, *7*, 208.
9. Jetbumpenkul, P.; Amornsudthiwat, P.; Kanopanont, S.; Damrongsakkul, S. *Int. J. Biol. Macromol.* **2012**, *50*, 7.
10. Liu, R.; Zhang, F.; Zuo, B. Q.; Zhang, H. X. *Adv. Mater. Res.* **2011**, *175*, 170.
11. Putthanarat, S.; Stribeck, N.; Fossey, S. A.; Eby, R. K.; Adams, W. W. *Polymer* **2000**, *41*, 7735.

12. Inoue, S. I.; Magoshi, J.; Tanaka, T.; Magoshi, Y.; Becker, M. J. *Polym. Sci. Part B: Polym. Phys.* **2000**, *38*, 1436.
13. Du, N.; Yang, Z.; Liu, X. Y.; Li, Y.; Xu, H. Y. *Adv. Funct. Mater.* **2011**, *21*, 772.
14. Giesa, T.; Arslan, M.; Pugno, N. M.; Buehler, M. *J. Nano Lett.* **2011**, *11*, 5038.
15. Lu, Q.; Zhu, H. S.; Zhang, C. C.; Zhang, F.; Zang, B.; Kaplan, D. L. *Biomacromolecules* **2012**, *13*, 826.
16. Nog, M.; Yano, H. *Adv. Mater.* **2008**, *20*, 1849.
17. Earland, C.; Raven, D. J. *Nature* **1954**, *174*, 461.
18. Rammensee, S.; Slotta, U.; Scheibel, T.; Bausch, A. R. *Proc. Natl. Acad. Sci. USA* **2008**, *105*, 6590.
19. Holland, C.; Terry, A. E.; Porter, D.; Vollrath, F. *Polymer* **2007**, *48*, 3388.
20. Chen, X.; Knight, D. P.; Shao, Z. Z.; Vollrath, F. *Polymer* **2001**, *42*, 9969.
21. Zhu, J. X.; Zhang, Y. P.; Shao, H. L.; Hu, X. C. *Polymer* **2008**, *49*, 2880.
22. Yoon, K.; Lee, H. N.; Ki, C. S.; Fang, D. F.; Hsiao, B. S.; Chu, B.; Um, I. C. *Int. J. Biol. Macromol.* **2013**, *61*, 50.
23. Zhang, K. H.; Mo, X. M.; Huang, C.; He, C. L.; Wang, H. S. *J. Biomed. Mater. Res. A* **2010**, *93*, 976.
24. Biesinger, M. C.; Lau, L. M.; Gerson, A. R.; Smart, R. C. *Appl. Surf. Sci.* **2010**, *257*, 887.
25. Jeong, L.; Lee, K. Y.; Liu, J. W.; Park, W. H. *Int. J. Biol. Macromol.* **2006**, *38*, 140.
26. She, Z. D.; Jin, C. R.; Huang, Z.; Zhang, B. F.; Feng, Q. L.; Xu, Y. X. *J. Mater. Med.* **2008**, *19*, 3545.
27. Chen, X.; Shao, Z. Z.; Marinkovic, N. S.; Miller, L. M.; Zhou, P.; Chance, M. R. *Biophys. Chem.* **2001**, *89*, 25.
28. Hu, X.; Kaplan, D. L.; Cebe, P. *Macromolecules* **2006**, *39*, 6161.
29. Chen, X.; Shao, Z. Z.; Knight, D.P.; Vollrath, F. *Proteins* **2007**, *68*, 223.
30. Lu, Q.; Wang, X. L.; Lu, S. Z.; Li, M. Z.; Kaplan, D. L.; Zhu, H. S. *Biomaterials* **2011**, *32*, 1059.
31. Chen, C.; Cao, C. B.; Ma, X. L.; Tang, Y.; Zhu, H. S. *Polymer* **2006**, *47*, 6322.
32. Zhou, J.; Cao, C. B.; Ma, X. L. *Int. J. Biol. Macromol.* **2009**, *45*, 504.
33. Lawrence, B. D.; Wharram, S.; Kluge, J. A.; Leisk, G. G.; Omenetto, F. G.; Rosenblatt, M. I.; Kaplan, D. L. *Macromol. Biosci.* **2010**, *10*, 393.
34. Lu, S. Z.; Wang, X. Q.; Lu, Q.; Zhang, X. H.; Kluge, J. A.; Uppal, N.; Omenetto, F.; Kaplan, D. L. *Macromolecules* **2010**, *11*, 143.
35. Zhang, C. C.; Song, D. W.; Lu, Q.; Hu, X.; Kaplan, D. L.; Zhu, H. S. *Macromolecules* **2012**, *13*, 2148.
36. Zhang, F.; Zuo, B. Q.; Fan, Z. H.; Xie, Z. G.; Lu, Q.; Zhang, X. G.; Kaplan, D. L. *Biomacromolecules* **2012**, *13*, 798.